Telomere shortening is a hallmark of genetic cardiomyopathies

Alex C. Y. Chang[a,b,c,d,e,1], Andrew C. H. Chang[a,b], Anna Kirillova[a,b], Koki Sasagawa[a,b], Willis Su[a,b], Gerhard Weber[a,b,c], Jue Lin[f], Vittavat Termglinchan[c], Ioannis Karakikes[c,g], Timon Seeger[c], Alexandra M. Dainis[c,h], John T. Hinson[i,j], Jonathan Seidman[k], Christine E. Seidman[i,k,l], John W. Day[m], Euan Ashley[c,d,e], Joseph C. Wu[c,n], and Helen M. Blau[a,b,c,1]

[a]Baxter Laboratory for Stem Cell Biology, Department of Microbiology and Immunology, Stanford University School of Medicine, Stanford, CA 94305; [b]Institute for Stem Cell Biology and Regenerative Medicine, Stanford University School of Medicine, Stanford, CA 94305; [c]Stanford Cardiovascular Institute, Stanford University School of Medicine, Stanford, CA 94305; [d]Stanford Center for Inherited Cardiovascular Disease, Stanford University School of Medicine, Stanford, CA 94305; [e]Division of Cardiovascular Medicine, Stanford University School of Medicine, Stanford, CA 94305; [f]Department of Biochemistry and Biophysics, School of Medicine, University of California, San Francisco, CA 94158; [g]Department of Cardiothoracic Surgery, Stanford University School of Medicine, Stanford, CA 94305; [h]Department of Genetics, Stanford University, Stanford, CA 94305; [i]Division of Cardiovascular Medicine, Brigham and Women's Hospital, Boston, MA 02115; [j]Cardiology Division, UConn Health and The Jackson Laboratory for Genomic Medicine, Farmington, CT 06032; [k]Department of Genetics, Harvard Medical School, Boston, MA 02115; [l]Howard Hughes Medical Institute, Chevy Chase, MD 20815; [m]Department of Neurology, Stanford University, Stanford, CA 94304; and [n]Department of Medicine, Division of Cardiology, Stanford University School of Medicine, Stanford, CA 94305

Contributed by Helen M. Blau, July 23, 2018 (sent for review August 17, 2017; reviewed by Dirk Hockemeyer and Charles E. Murry)

This study demonstrates that significantly shortened telomeres are a hallmark of cardiomyocytes (CMs) from individuals with end-stage hypertrophic cardiomyopathy (HCM) or dilated cardiomyopathy (DCM) as a result of heritable defects in cardiac proteins critical to contractile function. Positioned at the ends of chromosomes, telomeres are DNA repeats that serve as protective caps that shorten with each cell division, a marker of aging. CMs are a known exception in which telomeres remain relatively stable throughout life in healthy individuals. We found that, relative to healthy controls, telomeres are significantly shorter in CMs of genetic HCM and DCM patient tissues harboring pathogenic mutations: *TNNI3*, *MYBPC3*, *MYH7*, *DMD*, *TNNT2*, and *TTN*. Quantitative FISH (Q-FISH) of single cells revealed that telomeres were significantly reduced by 26% in HCM and 40% in DCM patient CMs in fixed tissue sections compared with CMs from age- and sex-matched healthy controls. In the cardiac tissues of the same patients, telomere shortening was not evident in vascular smooth muscle cells that do not express or require the contractile proteins, an important control. Telomere shortening was recapitulated in DCM and HCM CMs differentiated from patient-derived human-induced pluripotent stem cells (hiPSCs) measured by two independent assays. This study reveals telomere shortening as a hallmark of genetic HCM and DCM and demonstrates that this shortening can be modeled in vitro by using the hiPSC platform, enabling drug discovery.

telomere | dilated cardiomyopathy | hypertrophy cardiomyopathy | hiPSC-CM

Genetic cardiomyopathy—hypertrophic and dilated—affects 1 in 500–2,500 people worldwide and is the leading indication for heart transplantation. Genetic hypertrophic cardiomyopathy (HCM) and dilated cardiomyopathy (DCM) are caused by mutations in proteins with a diverse range of functions (1, 2). Genetic HCM is characterized by ventricular wall thickening, whereas DCM is characterized by dilation of the ventricular chamber. Patient outcomes range from reduced quality of life as a result of heart failure to sudden cardiac death between the ages of 20 and 60 y (3). Given this dismal prognosis, there is a great need for biomarkers and therapeutic targets common to HCM and DCM of diverse genetic etiologies.

Here, we show that telomere length constitutes such a biomarker. Telomeres are DNA sequences composed of (TTAGGG) repeats that serve as protective caps at the ends of chromosomes. Telomeres shorten at every cell division as a result of replication insufficiency and are markers of cellular aging. In contrast to most cell types, in healthy postnatal cardiomyocytes (CMs), telomeres are largely maintained throughout life (4, 5), presumably because postnatal CMs are relatively nonproliferative (6).

We first implicated telomere attrition in DCM in studies of Duchenne muscular dystrophy (DMD) (7, 8). We found that, although the mdx transgenic mouse, like patients with DMD, lacks dystrophin, it does not exhibit cardiac symptoms typical of DCM or premature death, a major conundrum for testing therapeutic strategies for DMD. We postulated that mice are protected from the disease by the lengths of their telomeres, which, for unknown reasons, are substantially longer than in humans. In support of this hypothesis, we "humanized" mdx mice to have shortened telomeres by breeding with the mTR-KO mouse that lacks telomerase activity as a result of the absence of the RNA component TERC (TR). Strikingly, the humanized mdx mice developed the severe skeletal muscle phenotype and heart failure seen in patients with DMD (7). We corroborated the findings in our mouse model (mdx^{4cv}/mTR^{G2}) in CMs of the hearts of patients with DMD, which exhibited, on average, a 48% decrease

Significance

We find that telomere shortening, which usually accompanies cell division in the course of aging, occurs in cardiomyocytes (CMs) of individuals with genetic hypertrophic cardiomyopathy (HCM) or dilated cardiomyopathy (DCM). HCM and DCM CMs differentiated from human-induced pluripotent stem cells (hiPSCs) also exhibit significant telomere shortening relative to healthy controls. By contrast, no telomere shortening was detected in vascular smooth muscle cells in tissue or hiPSC-derived cells, a cell type that does not express the mutant proteins. Our findings provide evidence for accelerated aging in CMs with familial cardiomyopathy. The potential to monitor the dynamics of telomere attrition in hiPSC-CMs over time will enable future mechanistic studies and screens for novel therapeutic agents to arrest telomere shortening and disease progression.

Author contributions: A.C.Y.C. and H.M.B. designed research; A.C.Y.C., A.C.H.C., A.K., K.S., W.S., G.W., J.L., V.T., I.K., T.S., A.M.D., and J.T.H. performed research; A.C.Y.C., A.C.H.C., A.K., K.S., W.S., G.W., J.L., V.T., I.K., T.S., A.M.D., J.T.H., and H.M.B. analyzed data; and A.C.Y.C., A.C.H.C., A.K., K.S., W.S., G.W., J.L., V.T., I.K., T.S., A.M.D., J.T.H., J.S., C.E.S., J.W.D., E.A., J.C.W., and H.M.B. wrote the paper.

Reviewers: D.H., Whitehead Institute for Biomedical Research; and C.E.M., University of Washington.

Conflict of interest statement: The sponsor declares a conflict of interest. J.L. is a cofounder and consultant to Telomere Diagnostics. The company played no role in this research.

[1]To whom correspondence may be addressed. Email: acychang@stanford.edu or hblau@stanford.edu.

Published online August 27, 2018.

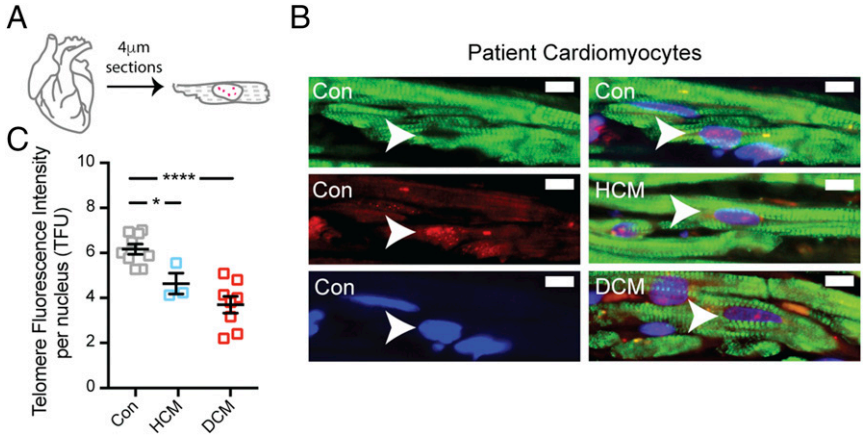

Fig. 1. HCM and DCM CMs exhibit telomere shortening. (*A*) Paraffin-embedded cardiac samples were used for telomere Q-FISH quantification of CMs. (*B*) Patient CMs [cardiac Troponin-T (green) indicated by white arrowhead] were stained for telomere (red) and for nuclear DAPI (blue) in patient and control cardiac tissue sections. (Scale bars, 10 μm.) Telomere levels were scored in a blinded fashion ($n = 40$–220 nuclei per patient tissue) within five to six regions of interest in two nonconsecutive sections, and (*C*) telomere signal intensity per DAPI-stained nucleus is plotted as mean ± SEM (*$P < 0.05$ and ****$P < 0.0001$).

in average telomere lengths relative to healthy controls. Notably, in contrast to CMs, contractile vascular smooth muscle cells (VSMCs) that do not express dystrophin had telomere lengths similar to control VSMCs in the mouse DMD model and Duchenne heart tissues, suggesting that the observed telomere shortening was specific to CMs and caused by the stress of contraction in the absence of the structural protein dystrophin (7, 8).

In this report, we test the hypothesis that telomere shortening is a general hallmark of genetic HCM and DCM as a result of mutations in contractile proteins essential to cardiac function. We measured telomeres in CMs from end-stage patient heart tissues at the time of heart transplantation and CMs derived from patient-induced pluripotent stem cells. Patient mutations included three genes associated with HCM [troponin I (*TNNI3*), cardiac myosin binding protein C (*MYBPC3*), and myosin heavy chain 7 (*MYH7*)] and three genes associated with DCM [dystrophin (*DMD*), cardiac troponin T (*TNNT2*), and titin (*TTN*)] (9–11). Relative to controls, in each case, significant telomere attrition was observed in diseased CMs from patients with DCM and HCM of diverse etiology.

Results

By using quantitative FISH (Q-FISH), we measured telomere fluorescence intensity per nucleus [in telomere fluorescence units (TFUs)] specifically in CMs expressing the CM-specific marker Troponin-T. Quantification entailed measurements with the use of a PNA probe against the telomere repeat normalized to nuclear DAPI in individual CMs in patient cardiac tissues for three HCM genotypes (*TNNI3*, *MYBPC3*,and *MYH7*) and for three DCM genotypes [*DMD* (7, 8), *TNNT2* (10), and *TTN* (12); Fig. 1 and Table 1]. In accordance with our findings in CMs in Duchenne tissues (7), the telomere levels of Troponin-T$^+$ CMs in HCM and DCM hearts were significantly reduced by, on average, 25% and 40%, respectively, compared with age- and sex-matched healthy controls (HCM, 4.64 ± 0.46 TFU, $P < 0.05$; DCM, 3.70 ± 1.05 TFU, $P < 0.0001$; control, 6.21 ± 0.16 TFU; Fig. 1*C*). Notably, VSMCs, a control cell type that neither expresses nor requires these contractile proteins, exhibited no telomere shortening in cardiac tissues of patients with HCM or DCM compared with healthy individuals (HCM, 4.91 ± 0.43 TFU; DCM, 4.52 ± 0.70 TFU; control, 4.68 ± 0.19 TFU, $P = 0.37$; Fig. 2). These data demonstrate that telomere shortening occurs in contractile CMs that have mutations in structural genes (*TNNI3*, *MYBPC3*, *MYH7*, *DMD*, *TNNT2*, and *TTN*).

To investigate whether the telomere shortening seen in CMs in tissues also occurs in a disease model of HCM and DCM in vitro, we compared telomere lengths in human-induced pluripotent stem cells (hiPSCs) differentiated into CMs (hiPSC-CMs). We generated hiPSCs from HCM and DCM patients' peripheral blood mononuclear cells using the four Yamanaka factors (13) and used a sequential regimen of growth factors to differentiate these cells into beating CMs (Fig. 3 *A* and *B*) by using well-established protocols (13, 14). Control hiPSC lines were from a healthy individual (Con#1), healthy family members (Con#2, Con#3 for TNNT2#1–3; Con#5 for TTN#2), or a CRISPR/Cas9-mediated corrected isogenic line (Con#4 for TTN#1; Table 1). Importantly, in all cases, we measured telomeres in hiPSC-CMs at day 30 of differentiation. The five HCM hiPSC-CMs (6.16 ± 0.65 TFU, $P < 0.0005$; Table 1, blue) and eight DCM hiPSC-CMs (5.70 ± 0.65 TFU, $P < 0.0001$; Table 1, red) exhibited significant 52% and 58% decreases in telomere levels, respectively, compared with the control hiPSC-CMs of diverse etiology (5.83 ± 0.65 TFU; Fig. 3*C*, gray triangle and gray squares; Table 1, gray). These data are also shown for each patient line separately (Fig. 3*C*).

To validate the telomere attrition by a second method, we employed a previously established quantitative PCR (qPCR) assay (15, 16). We enriched for hiPSC-CMs in the highly heterogeneous cell cultures by FACS for mitochondrial content assessed by tetramethylrhodamine methyl ester (TMRM; perchlorate) staining as previously described (Fig. 3*D*) (14). We used RT-qPCR to verify that the TMRM$^+$ population was enriched for CM markers NKX2.5, TNNI3, and TNNT2 (Fig. 3*E*). By contrast, the TMRM$^-$ population was enriched for smooth muscle, endothelial, and fibroblast markers VIM, CDH5, and FSP1, respectively (Fig. 3*E*). Relative telomere amounts (i.e., T/S ratios) were determined by qPCR, quantified as the telomere amplification cycle (T) relative to the amplification cycle of a single copy gene (S) (15, 16). The T/S ratios in HCM and DCM TMRM$^+$ CMs were significantly reduced by, on average, 21% and 39%, respectively, compared with control CMs (HCM, 2.67 ± 0.18, $P < 0.05$; DCM, 2.06 ± 0.16, $P < 0.0005$; control, 3.40 ± 0.24; Fig. 3*F*). As a control cell type, we analyzed telomere lengths in hiPSCs differentiated into VSMCs (hiPSC-VSMCs) by using an established protocol (17). In accordance with the VSMCs in patient tissues, no significant difference in telomeres were detected between control, HCM, and DCM smooth muscle actin-positive hiPSC-VSMCs (control, 4.93 ± 0.43; HCM, 4.84 ± 0.48; DCM, 4.29 ± 0.15, $P = 0.35$; Fig. 4).

Table 1. Patient cardiac and hiPSC lines used

Classification	Patient/line	Gene	Age, y	Sex	Source	Q-FISH (*n*)
Human cardiac samples						
Healthy	Con#1	NA	35	Male	University of British Columbia	70
Healthy	Con#2	NA	21	Male	University of British Columbia	69
Healthy	Con#3	NA	21	Male	University of British Columbia	65
Healthy	Con#4	NA	47	Male	University of British Columbia	124
Healthy	Con#5	NA	41	Male	University of British Columbia	128
Healthy	Con#6	NA	32	Male	University of British Columbia	121
Healthy	Con#7	NA	49	Female	University of British Columbia	99
Healthy	Con#8	NA	53	Female	University of British Columbia	214
Healthy	Con#9	NA	54	Female	University of British Columbia	220
HCM	TNNI3	TNNI3 (p.Arg186Gln)	60	Male	Stanford University	72
HCM	MYBPC3	MYBPC3 (IVS11-9G > A)	25	Female	Stanford University	36
HCM	MYH7	MYH7 (p.Ala26Val)	56	Female	Stanford University	32
DCM	DMD#1	DMD	13	Male	Harvard University	42
DCM	DMD#2	DMD	15	Male	Harvard University	94
DCM	DMD#3	DMD	17	Male	Johns Hopkins University	65
DCM	DMD#4	DMD	19	Male	University of Wisconsin	72
DCM	TNNT2	TNNT2 (p.R173W)	15	Male	Stanford University	804
DCM	Titin#1	TTN (c.92569+1G > C)	40	Male	Harvard University	245
DCM	Titin#2	TTN (c.44725+2delT)	50	Male	Harvard University	113
DCM	Titin#3	TTN (26211W>*stop)	50	Male	Harvard University	55
Patient hiPSC lines						
Healthy	Con#1	Healthy control	45	Male	Stanford University	92
Healthy	Con#2	Family control from TNNT2	16	Male	Stanford University	40
Healthy	Con#3	Family control from TNNT2	77	Male	Stanford University	44
Healthy	Con#4	Isogenic control of TTN#1	62	Male	Harvard University	100
Healthy	Con#5	Family control from TTN#2	48	Female	Harvard University	210
HCM	MYBPC3#1	MYBPC3 (R943x)	29	Male	Stanford University	519
HCM	MYH7#1	MYH7 (R723C)	32	Male	Stanford University	115
HCM	MYH7#2	MYH7 (R403Q)	45	Female	Stanford University	79
HCM	MYH7#3	MYH7 (R719W)	34	Male	Stanford University	54
HCM	MYH7#4	MYH7 (R663H)	57	Male	Stanford University	37
DCM	DMD#1	DMD (c.3638_3650del)	6	Male	Stanford University	129
DCM	DMD#2	DMD (c.6599 C > G)	12	Male	Stanford University	48
DCM	DMD#3	DMD (c.9204_9207del)	9	Male	Stanford University	164
DCM	TNNT2#1	TNNT2 (p.R173W)	45	Male	Stanford University	117
DCM	TNNT2#2	TNNT2 (p.R173W)	39	Male	Stanford University	131
DCM	TNNT2#3	TNNT2 (p.R173W)	15	Male	Stanford University	50
DCM	TTN#1	TTN (cN22577fs$^{+/-}$)	62	Male	Harvard University	184
DCM	TTN#2	TTN (c.67745delT)	15	Male	Harvard University	133

NA, not applicable.

Discussion

Our data implicate telomere shortening as a hallmark of genetic cardiomyopathies evident in CMs of patient cardiac tissues and patient CMs derived from hiPSCs. This shortening occurs when human mutations are present, e.g., *DMD*, *MYBPC3*, *MYH7*, *TNNT2*, *TNNI3*, and *TTN*, that encode proteins crucial to CM function. These findings were unexpected, as adult human CMs are characterized by low cell turnover (4, 6) and telomere lengths do not change in healthy individuals with aging (4). Remarkably, we observed similar telomere shortening in patient hiPSC-CMs, although these cells are known to be relatively immature CMs (14). We corroborated this shortening for patient hiPSC-CMs by two independent methods, Q-FISH analysis of single CMs (telomere signal relative to nuclear signal) and qPCR of FACS-enriched CM populations (telomere signal relative to single-copy gene signal). These two methods provide distinct measures of the reduction in relative telomere lengths. The robustness of our findings is underscored by the fact that the hiPSCs were derived and differentiated in different laboratories, yet remarkably similar, statistically significant results were obtained across genotypes. Moreover, the control hiPSC-CMs exhibited strikingly similar telomere levels regardless of whether they were from a healthy control subject, unaffected relatives, or isogenic CRISPR/Cas9-mediated corrected counterparts.

Our report suggests that telomere shortening plays a role in the etiology and progression of genetic cardiomyopathies and establishes the hiPSC system as a way to model this shortening in patient CMs differentiated in culture. A prior report demonstrated by Southern blot analysis that telomeres are significantly shorter in cardiac tissues from patients who die of heart failure relative to normal individuals (18). By using Q-FISH, telomere attrition was reported in CMs of HCM patient tissues (19). Additionally, telomere lengths have been shown to be heterogeneous in cells of cardiac tissues of aged mice (20). Finally, in mice with systemic genetically induced short telomeres caused by absence of TERC (mTR^{G4}), CM exit from the cell cycle and expression of p21 was accelerated and evident at birth (21) and the mice died of dilated cardiomyopathy.

Two reports now strongly suggest that mice are protected from human cardiac disease by the length of their telomeres. Dilated

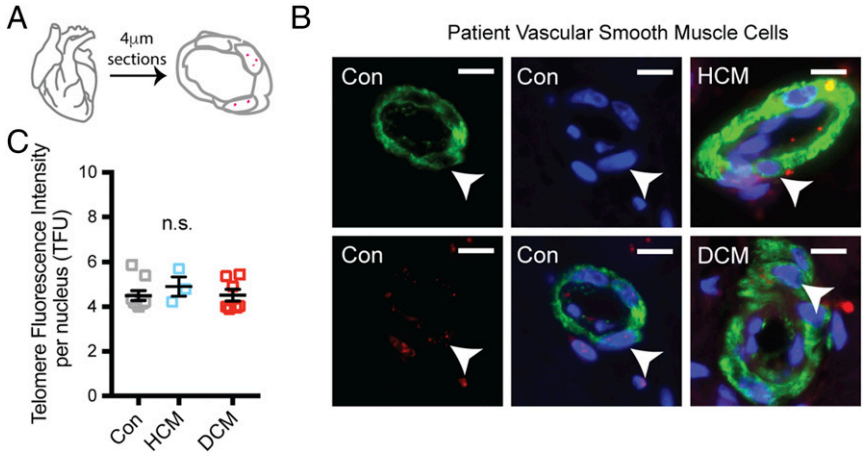

Fig. 2. HCM and DCM VSMCs do not exhibit telomere shortening. (*A*) Paraffin-embedded cardiac samples were used for telomere Q-FISH quantification of VSMCs. (*B*) Patient VSMCs [smooth muscle actin (green) indicated by white arrowhead] were stained for telomere (red) and for nuclear DAPI (blue) in patient and control cardiac tissue sections. (Scale bars, 10 μm.) Telomere levels were scored in a blinded fashion (n = 30–150 nuclei per patient tissue) within three to four regions of interest in two nonconsecutive sections, and (*C*) telomere signal intensity per DAPI-stained nucleus is plotted as mean ± SEM.

cardiomyopathy was not evident in the murine model of DMD (mdx) until the telomeres were humanized, that is, somewhat shortened ubiquitously by breeding to the mTR-KO mouse (mdx/mTR^{G4}) (7, 8). Similarly, the human aortic valve stenosis caused by calcification in patients with haploinsufficiency for Notch was not apparent in mice until their telomeres were shortened ($N1^{+/-}$ mTR^{G2}) (22).

How telomere shortening impacts cardiac function remains unknown. Mitochondrial dysfunction likely plays a significant role, as mice with systemic critically short telomeres (mTR^{G4}) exhibit decreased expression of the master mitochondrial regulator PGC1a and have reduced mitochondrial content (23), as does the Duchenne mdx/mTR^{G2} mouse model (8). These murine models suggest that a telomere–mitochondrial axis is key to maintaining cardiac function and, in its absence, dilated cardiomyopathy leading to heart failure ensues (22, 23).

The mechanism by which telomeres shorten in nonproliferative CMs is also subject to debate. One possibility is that telomere ends are "deprotected" as a result of mechanical stress. In support of this hypothesis, failing patient hearts exhibit short telomeres and decreased expression of Telomeric repeat-binding factor 2 (TERF2), a shelterin protein that binds to and protects telomeric ends (18). Another possibility is that the accumulation of reactive oxygen species (ROS) presages telomere shortening. In Duchenne murine CMs, aberrant contraction has been shown to lead to increased ROS (8, 24). Moreover, elevated ROS levels in confluent nonproliferating fibroblasts exposed to hyperoxia have been shown to correlate with telomere shortening (25). A telomere position effect has been described to account for interactions detected by chromosome capture followed by high-throughput sequencing of distal promoter and telomere regions in cultured vascular endothelial cells. This interaction dictates gene expression, and is lost in aged endothelium (26). Conversely, telomerase expression is beneficial. Telomerase activity is induced in mice that exercise (27), and overexpression of telomerase protein (TERT) in mouse CMs protects the animals from myocardial infarction (28, 29) by an unknown mechanism. It is tempting to postulate that the telomere position effect is at play in aortic valve disease, as Notch is located proximal to the telomere in humans (22). For DCM and HCM CMs, to elucidate the effect of short telomeres on cardiac function, gene expression and gain- and loss-of-function studies are warranted. Taken together, these data suggest that telomeres play an important role in cardiovascular homeostasis.

The hiPSC-CM disease model culture system used here now affords a unique opportunity to resolve the mechanisms by which CM telomeres shorten as a result of protein insufficiency. Moreover, this system enables identification of previously uncharacterized modes of therapeutic intervention. Although a larger cohort is necessary to provide conclusive findings, our data provide tantalizing evidence in support of telomere shortening as a biomarker of premature CM aging in genetic HCM and DCM cardiomyopathies.

Materials and Methods

Statistical differences in primary patient samples and between the hiPSC and hiPSC-CM groups were analyzed by one-way ANOVA tests by comparing the mean of each group with the mean of every other group, followed by Holm–Šídák multiple comparison test. Image capture and telomere quantification analyses were performed in a blinded fashion to avoid bias. All data are shown as the mean ± SEM. Significant differences were determined as those with $P < 0.05$.

Human Cardiac Samples. All protocols that used human samples were reviewed and approved by the Stanford Institutional Review Board (no. 13465). Control hearts were isolated <24 h post mortem from deidentified male patients who died of noncardiac disease at University of British Columbia. The TNNT2 DCM patient cardiac tissue sample and the HCM patient cardiac samples were obtained from explanted heart tissues from patients with end-stage cardiomyopathy just before heart transplantation at Stanford University. The TTN DCM patient cardiac tissue samples were from Harvard University (12), and the DMD DCM patient cardiac tissue samples were from Harvard University, Johns Hopkins University, and the University of Wisconsin as previously described (7). All tissue samples were subjected to formalin fixation, pH 7.0, followed by paraffin embedding. Sections (4 μm) from paraffin blocks were placed on ChemMate slides (Fisher Scientific) for telomere Q-FISH analyses as previously described (7, 8).

Culture of hiPSCs and Cardiac and Smooth Muscle Cell Differentiation. All protocols that used human iPSCs were reviewed and approved by the Stanford Stem Cell Research Oversight committee (no. 602). Human hiPSCs were grown on Matrigel-coated plates using chemically defined mTeSR1 or Nutristem medium as previously described (30). The medium was changed daily, and cells were passaged every 4 d by using EDTA. hiPSCs were grown to 70–90% confluence and subsequently differentiated subsequently into beating CMs as described previously (30). Briefly, hiPSC were treated with a Wnt activator CHIR-99021 (4–6 μM; Selleck Chem) for 2 d, followed by a Wnt inhibitor IWR-1 (5 μM; Sigma) for 2 d, both in RPMI 1640 medium supplemented with B27 minus insulin (Thermo Fisher Scientific). Cells were allowed to recover in fresh RPMI 1640 medium supplemented with B27 minus insulin for 2 d before switching to RPMI 1640 medium supplemented with B27 for 4 d. Beating hiPSC-CMs were purified and maintained in glucose-free conditions by using RPMI 1640 medium without glucose with B27 supplement

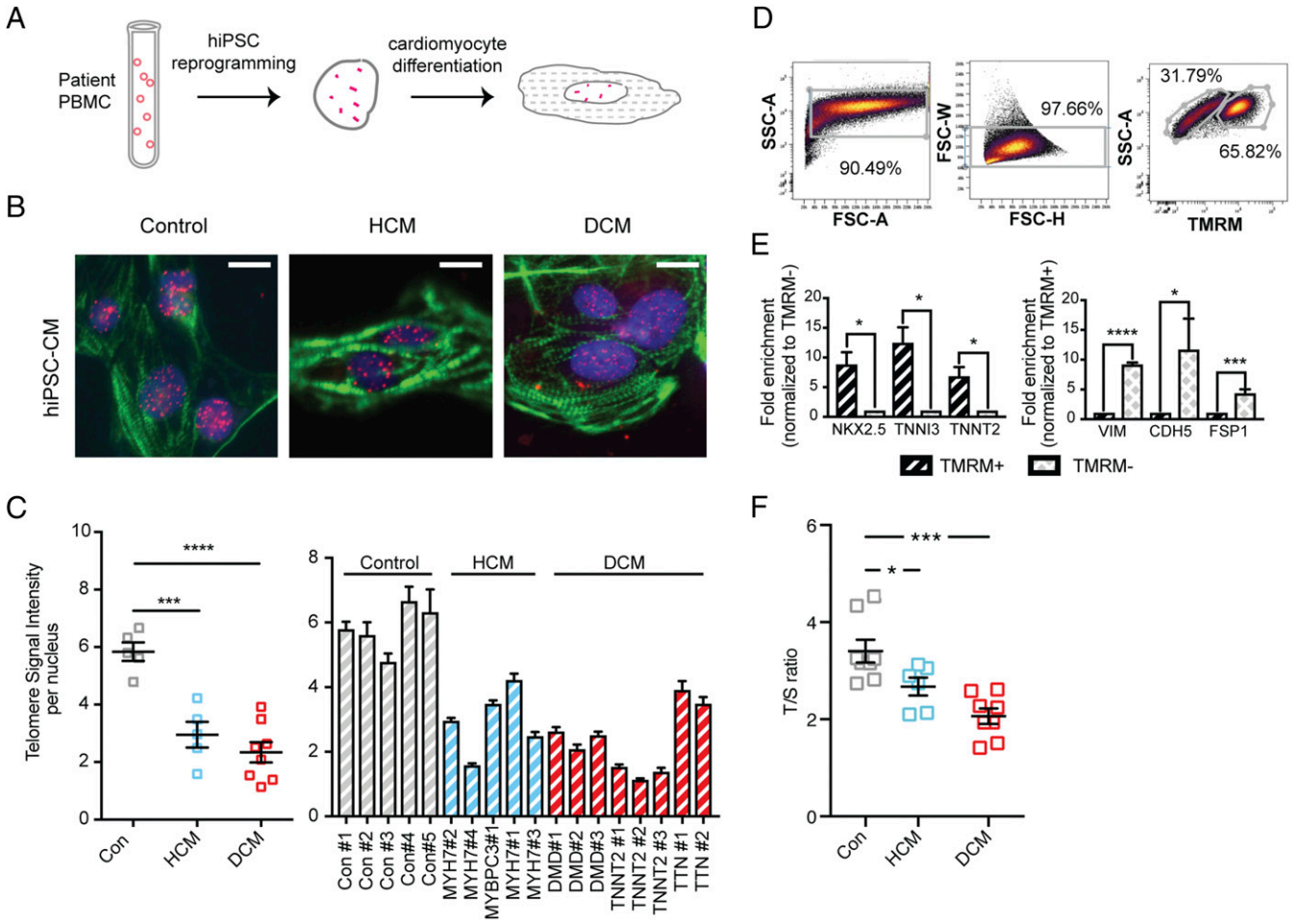

Fig. 3. HCM and DCM hiPSC-derived CMs recapitulate telomere shortening. (*A*) Patient PBMCs were used to generate patient-specific hiPSC lines and used to differentiate into hiPSC-CMs. (*B*) Cardiomyopathic patient and control day 30 hiPSC-CMs were used to assess telomere levels. Representative hiPSC-CMs (cardiac Troponin-T; green) were stained for telomeres (red) and nuclear DAPI (blue). (Scale bars, 10 μm.) (*C*) Telomere signal intensity per DAPI-stained nucleus is shown for HCM, DCM, and control hiPSCs (day 0) and hiPSC-CMs (day 30). hiPSC differentiation was performed in two independent experiments per line from the same passage cells, and telomere levels were scored in a blinded fashion (n = 40–330 nuclei per hiPSC or hiPSC-CM). (*D*) FACS gating for TMRM sorting. (*E*) TMRM$^+$ population enriched for CM markers whereas TMRM$^-$ population enriched for non-CM markers by RT-qPCR (TMRM$^+$, n = 5; TMRM$^-$, n = 3). (*F*) Telomere T/S ratio is shown for HCM (n = 6), DCM (n = 8), and control (n = 8) TMRM$^+$ hiPSC-CMs (day 30). All data plotted as mean ± SEM (*P < 0.05, ***P < 0.001, and ****P < 0.0001).

and 4 mM lactate (Life Technologies) until day 30 to favor metabolic maturation, as previously described (30). For hiPSC-SMCs, hiPSCs were seeded onto collagen IV (BD Biosciences)-coated plates in Nutristem medium and subsequently differentiated into VSMCs by using the PDGF-BB and TGFB1 (R&D Systems) method as previously described (17).

Telomere Q-FISH, Immunofluorescence Microscopy, and Image Acquisition. Cardiac paraffin sections were deparaffinized in xylene and rehydrated in serial ethanol concentrations (7). All samples were fixed with 4% paraformaldehyde in PBS solution for 5 min at room temperature and subsequently maintained in PBS solution at 4 °C. hiPSCs were fixed on day 0; hiPSC-CMs were cultured in differentiation medium, reseeded on day 27 onto Matrigel-coated eight-chamber slides, and fixed on day 30 of differentiation; and hiPSC-VSMCs were reseeded on day 12 and fixed on day 14 of differentiation. Telomere Q-FISH was performed as previously described by using TelC-Cy3 PNA probe (CCCTAACCCTAACCCTAA; F1002; PNA Bio) (7, 8). Tissues were blocked with staining buffer (4% calf serum/0.1%Triton X-100/PBS solution) and stained with prediluted mouse antibody to cardiac troponin-T (ab74275; Abcam) for 2 h at room temperature or rabbit antibody to smooth muscle actin (ab32575; Abcam) overnight at 4 °C in staining buffer, washed with PBS solution, incubated with goat anti-mouse or anti-rabbit Alexa 488 (1:400; Abcam) for 1 h, and counterstained with 1 μg·mL^{-1} DAPI in PBS solution for 5 min, washed with distilled H_2O, air-dried, and mounted with ProLong Gold Antifade (Life Technologies). Images were captured on a Nikon spinning-disk confocal microscope by using a PLAN APO 40× objective. Telomere signal intensity was determined as PNA signal normalized to nuclear DAPI (in TFU) in Troponin-T$^+$ CMs or α-smooth muscle actin$^+$ VSMCs and captured by using the ImageJ plugin Telometer as previously described (7, 8).

FACS Purification. Cell cultures were dissociated by using Accutase (Thermo Fisher Scientific) and stained with 50 nM TMRM according to the established protocol (14). Cells were gated for side scatter and forward scatter to avoid debris and doublets, and TMRM$^+$ (CMs) and TMRM$^-$ (non-CMs) were isolated for downstream characterization.

Telomere Measurement by qPCR. Genomic DNA was purified from cell pellets (≥500,000 TMRM$^+$ hiPSC-CMs) stored at −80 °C by using a QIAamp DNA mini kit (Qiagen) and quantified by measuring OD_{260}. DNA quality control criteria were an OD_{260}/OD_{280} between 1.7 and 2.0. The telomere length measurement assay was adapted from the published original method by Cawthon (15, 16, 30). The telomere PCR primer tel1b [5′-CGGTTT(GTTTGG)5GTT-3′] was used at 100 nM concentration, and tel2b [5′-GGCTTG(CCTTAC)5CCT-3′] was used at 900 nM concentration. The single-copy gene PCR primer (human β-globin) hbg1 [5′ GCTTCTGACACAACTGTGTTCACTAGC-3′] was used at 300 nM, and hbg2 [5′-CACCAACTTCATCCACGTTCACC-3′] was used at 700 nM concentration. The final reaction mix contained 20 mM Tris·HCl, pH 8.4, 50 mM KCl, 200 μM each dNTP, 1% DMSO, 0.4× SYBR Green I, 22 ng *Escherichia coli* DNA per

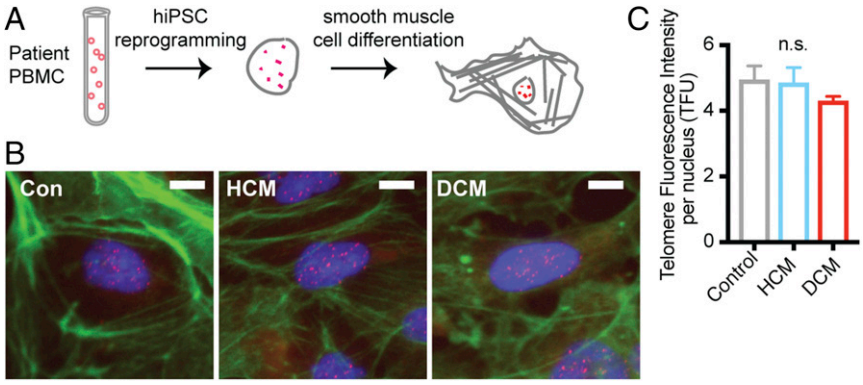

Fig. 4. HCM and DCM hiPSC-derived VSMCs do not exhibit telomere shortening. (*A*) Patient PBMCs were used to generate patient-specific hiPSC lines and used to differentiate into hiPSC-VSMCs. (*B*) Cardiomyopathic patient and control day 14 hiPSC-VSMCs were used to assess telomere signals. Representative hiPSC-VSMCs (smooth muscle actin; green) were stained for telomere signal (red) and nuclear DAPI (blue). (Scale bars, 10 μm.) (*C*) Telomere signal intensity per DAPI-stained nucleus is shown for HCM, DCM, and control hiPSC-VSMCs. hiPSC-VSMC differentiation was performed in two independent experiments from the same passage cells, and telomere TFUs were scored in a blinded fashion (n = 36–49 nuclei per group) and plotted as mean ± SEM.

reaction, 0.4 U Platinum Taq DNA polymerase (Invitrogen), and 3–6 ng of genomic DNA per 11-μL reaction. Tubes containing 26, 8.75, 2.9, 0.97, 0.324, and 0.108 ng of a reference DNA (cat. no. G152A; Promega) were included in each PCR run as a standard curve to determine the quantity of targeted templates in each research sample. The same reference DNA was used for all PCR runs. All samples were run in triplicate wells. The averages of T and S concentrations from the triplicate wells were used to calculate the T/S ratios. To control for interassay variability, eight control DNA samples were included in each run. The T/S ratio of each control DNA is divided by the average T/S ratio for the same DNA from 10 runs to get a normalizing factor. This was done for all eight control DNA samples, and the average normalizing factor for all eight samples was used to correct the unknown DNA samples to obtain the final T/S ratio. The T/S ratio for each sample was measured twice, and the average of the two values were used as the final data.

ACKNOWLEDGMENTS. We thank John Ramunas for his comments and suggestions, Dr. Michael Seidman (Cardiovascular Tissue Registry, Centre for Heart Lung Innovation, Providence Health Care, University of British Columbia) for providing the control cardiac tissues, Jon Mulholland and Cedric Espenel for expert microscopy assistance in the Nikon Spinning Disk Confocal microscope (funded jointly by the School of Engineering and the Beckman Center), and Colin Holbrook for his help with FACS sorting. This research was supported by American Heart Association Grants 13POST14480004 and 18CDA34110411 (to A.C.Y.C.), 15BGIA22730027 (to I.K.), 17MERIT33610009 (to J.C.W.), and 17CSA33590101 (to H.M.B.); the Stanford School of Medicine Dean's Fellowship (to A.C.Y.C.); Canadian Institutes of Health Research Fellowship Grant 201411MFE-338745-169197 (to A.C.Y.C.); a Stanford Cardiovascular Institute Seed Grant (to I.K. and A.C.Y.C.); the National Science Foundation Graduate Research Fellowship Program (A.M.D.); the Stanford–Coulter Translational Research Grant Program (A.M.D.); Burroughs Wellcome Fund Innovation in Regulatory Science Award 1015009 (to J.C.W.); National Institutes of Health Grants K99 HL104002 (to I.K.), K08 HL125807 (to J.T.H.), and R01 HL126527, R01 HL130020, R01 HL123968, and R24 HL117756 (to J.C.W.); the German Research Association/Deutsche Forschungsgemeinschaft (T.S.); the Howard Hughes Medical Institute (C.E.S.); the Baxter Foundation (H.M.B.); and National Institutes of Health Grants AG044815 and AR063963 (to H.M.B.).

1. Booth SA, Charchar FJ (2017) Cardiac telomere length in heart development, function, and disease. *Physiol Genomics* 49:368–384.
2. Parvari R, Levitas A (2012) The mutations associated with dilated cardiomyopathy. *Biochem Res Int* 2012:639250.
3. Force T, et al. (2010) Research priorities in hypertrophic cardiomyopathy: Report of a Working Group of the National Heart, Lung, and Blood Institute. *Circulation* 122: 1130–1133.
4. Takubo K, et al. (2002) Telomere lengths are characteristic in each human individual. *Exp Gerontol* 37:523–531.
5. Terai M, et al. (2013) Association of telomere shortening in myocardium with heart weight gain and cause of death. *Sci Rep* 3:2401.
6. Bergmann O, et al. (2009) Evidence for cardiomyocyte renewal in humans. *Science* 324:98–102.
7. Mourkioti F, et al. (2013) Role of telomere dysfunction in cardiac failure in Duchenne muscular dystrophy. *Nat Cell Biol* 15:895–904.
8. Chang ACY, et al. (2016) Telomere shortening and metabolic compromise underlie dystrophic cardiomyopathy. *Proc Natl Acad Sci USA* 113:13120–13125.
9. Lan F, et al. (2013) Abnormal calcium handling properties underlie familial hypertrophic cardiomyopathy pathology in patient-specific induced pluripotent stem cells. *Cell Stem Cell* 12:101–113.
10. Sun N, et al. (2012) Patient-specific induced pluripotent stem cells as a model for familial dilated cardiomyopathy. *Sci Transl Med* 4:130ra47.
11. Wu H, et al. (2015) Epigenetic regulation of phosphodiesterases 2A and 3A underlies compromised β-adrenergic signaling in an iPSC model of dilated cardiomyopathy. *Cell Stem Cell* 17:89–100.
12. Herman DS, et al. (2012) Truncations of titin causing dilated cardiomyopathy. *N Engl J Med* 366:619–628.
13. Burridge PW, Keller G, Gold JD, Wu JC (2012) Production of de novocardiomyocytes: Human pluripotent stem cell differentiation and direct reprogramming. *Cell Stem Cell* 10:16–28.
14. Tohyama S, et al. (2013) Distinct metabolic flow enables large-scale purification of mouse and human pluripotent stem cell-derived cardiomyocytes. *Cell Stem Cell* 12: 127–137.
15. Cawthon RM (2009) Telomere length measurement by a novel monochrome multiplex quantitative PCR method. *Nucleic Acids Res* 37:e21.
16. Cawthon RM (2002) Telomere measurement by quantitative PCR. *Nucleic Acids Res* 30:e47.
17. Wanjare M, Kuo F, Gerecht S (2013) Derivation and maturation of synthetic and contractile vascular smooth muscle cells from human pluripotent stem cells. *Cardiovasc Res* 97:321–330.
18. Oh H, et al. (2003) Telomere attrition and Chk2 activation in human heart failure. *Proc Natl Acad Sci USA* 100:5378–5383.
19. Sharifi-Sanjani M, et al. (2017) Cardiomyocyte-specific telomere shortening is a distinct signature of heart failure in humans. *J Am Heart Assoc* 6:e005086.
20. Rota M, et al. (2007) The young mouse heart is composed of myocytes heterogeneous in age and function. *Circ Res* 101:387–399.
21. Aix E, Gutiérrez-Gutiérrez Ó, Sánchez-Ferrer C, Aguado T, Flores I (2016) Postnatal telomere dysfunction induces cardiomyocyte cell-cycle arrest through p21 activation. *J Cell Biol* 213:571–583.
22. Theodoris CV, et al. (2017) Long telomeres protect against age-dependent cardiac disease caused by NOTCH1 haploinsufficiency. *J Clin Invest* 127:1683–1688.
23. Sahin E, et al. (2011) Telomere dysfunction induces metabolic and mitochondrial compromise. *Nature* 470:359–365.
24. Prosser BL, Ward CW, Lederer WJ (2011) X-ROS signaling: Rapid mechano-chemo transduction in heart. *Science* 333:1440–1445.
25. Sitte N, Saretzki G, von Zglinicki T (1998) Accelerated telomere shortening in fibroblasts after extended periods of confluency. *Free Radic Biol Med* 24:885–893.
26. Robin JD, et al. (2014) Telomere position effect: Regulation of gene expression with progressive telomere shortening over long distances. *Genes Dev* 28:2464–2476.
27. Werner C, et al. (2009) Physical exercise prevents cellular senescence in circulating leukocytes and in the vessel wall. *Circulation* 120:2438–2447.
28. Oh H, et al. (2001) Telomerase reverse transcriptase promotes cardiac muscle cell proliferation, hypertrophy, and survival. *Proc Natl Acad Sci USA* 98:10308–10313.
29. Bär C, et al. (2014) Telomerase expression confers cardioprotection in the adult mouse heart after acute myocardial infarction. *Nat Commun* 5:5863.
30. Hinson JT, et al. (2015) HEART DISEASE. Titin mutations in iPS cells define sarcomere insufficiency as a cause of dilated cardiomyopathy. *Science* 349:982–986.